EFFECTS OF VARIABLE VISCOSITY AND THERMAL CONDUCTIVITY ON UNSTEADY MHD FLOW OF NON-NEWTONIAN FLUID OVER A STRETCHING POROUS SHEET

by

Gamal M. ABDEL-RAHMAN

Department of Mathematics, Faculty of Science, Benha University, Benha, Egypt

Original scientific paper
DOI: 10.2298/TSCI110529025R

The unsteady flow and heat transfer in an incompressible laminar, electrically conducting and non-Newtonian fluid over a non-isothermal stretching sheet with the variation in the viscosity and thermal conductivity in a porous medium by the influence of an external transverse magnetic field have been obtained and studied numerically. By using similarity analysis the governing differential equations are transformed into a set of non-linear coupled ordinary differential equations which are solved numerically. Numerical results were presented for velocity and temperature profiles for different parameters of the problem as power law parameter, unsteadiness parameter, radiation parameter, magnetic field parameter, porous medium parameter, temperature buoyancy parameter, Prandtl parameter, modified Eckert parameter, Joule heating parameter, heat source/sink parameter, and others. A comparison with previously published work has been carried out and the results are found to be in good agreement. Also the effects of the pertinent parameters on the skin friction and the rate of heat transfer are obtained and discussed numerically and illustrated graphically.

Key words: *unsteady flow, non-Newtonian fluid, magnetohydrodynamics, porous medium*

Introduction

Many industrial fluids as the non-linear fluid rheology become of special interest and have practical applications. Hence the study of non-Newtonian fluid flow is important, different models have been proposed to explain the behaviour of non-Newtonian fluid. Among these, the power law, the differential type, and the rate type models gained importance. The knowledge of flow and heat mass transfer within a thin liquid film is crucial in understanding the coating process, designing of heat exchangers and chemical processing equipments. This interest stems from many engineering and geophysical applications such as geothermal reservoirs and other applications including wire and fibre coating, food stuff processing, reactor fluidization, transpiration cooling, thermal insulation, enhanced oil recovery, packed bed catalytic reactors, cooling of nuclear reactors and underground energy transport. The prime aim in almost every extrusion is to maintain the surface quality of the extricate. All coating processes demand a smooth glossy surface to meet the requirements for the best appearance and optimum service properties such as low friction, transparency and strength.

Present address: Department of Mathematics, Faculty of Science, Princess Norah Bint Abdelrahman University, Riyadh, Kingdom of Saudi Arabia
* Corresponding author; e-mail: gamalm60@yahoo.com

Also, many metallurgical processes involve the cooling of continuous strips or filaments by drawing them through a quiescent fluid, and in the process of drawing, these strips are stretched. This type of flow was firstly initiated by Sakiadis [1] for moving an inextensible sheet and later extended by Crane [2] to fluid flow over a linearly stretched sheet.

Thereafter, numerous investigations were done on the stretching sheet problem with linear stretching in different directions [3-8]. All the above studies restrict their analysis to Newtonian flows in the absence of the magnetic field. In recent years, it has been observed that a number of industrial fluids such as molten plastics, artificial fibers, polymeric liquids, blood, food stuff, and slurries exhibit non-Newtonian fluid behavior. It may also be pointed out that, many industrial processes involve the cooling of continuous strips or filaments by drawing them through a quiescent fluid. During this process, these strips are sometimes stretched. In all these cases, the properties of the final product depend to a great extent on the rate of cooling. By drawing such strips in an electrically conducting fluid subjected to a uniform magnetic field, the rate of cooling can be controlled and the desired characteristics of the final product can be obtained. Another important application of hydromagnetic flows to metallurgy lies in the purification of molten metal's from non-metallic inclusion by the application of magnetic field. In view of these applications, Sarpakaya [9] was the first among others to study the magnetohydrodynamic (MHD) flow of non-Newtonian fluids. This work was later extended by many authors by considering the non-Newtonian visco-elastic flow, heat and mass transfer under different physical situations [10-16]. It is worth mentioning here that many inelastic non-Newtonian fluids, encountered in chemical engineering processes, are known to follow the empirical Ostwald-de Waele so called "power law model". This model is described by a simple non-linear equation of state for inelastic fluids which includes linear Newtonian fluids as a special case.

The power law model provides an adequate representation of many non-Newtonian fluids over the most important range of shear stress. Although this model merely shows an empirical relationship between the stress and velocity gradients, it has been successfully applied to non-Newtonian fluids experimentally. The two constants in the model can be chosen with great ease for specific fluids and the model is found to be good in representing pseudo-plastic behavior. It is frequently used in oil engineering. A considerable amount of work has been done in this field by taking into account the heat and mass transfer. Schowalter [17] has introduced the concept of boundary layer theory of non-Newtonian fluids. Acrivos *et al.* [18] have investigated the steady laminar flow of non-Newtonian fluids over a plate. Lee and Ames [19] extended the above work to find the similarity solutions for non-Newtonian power law fluid. Andersson *et al.* [20] studied the boundary layer flow of an electrically conducting incompressible fluid obeying the power law model, in the presence of transverse magnetic field. Howell *et al*. [21] examined the momentum and heat transfer occurring in the laminar boundary layer on a continuously moving and stretching surface in a non-Newtonian power law fluid. However all these studies are restricted to the analysis of either flow characteristics or flow and heat transfer characteristics over an impervious stretching boundary. We know that the characteristic properties of the final product of the material depend to a great extent on the rate of cooling through the adjacent boundary. The rate of cooling associated with the heat transfer phenomena may be controlled by suction/blowing through the porous boundary in the presence of a constant transverse magnetic field. Hassanien *et al.* [22] presented a work on flow and heat transfer in power law fluid over a stretching porous surface with variable surface temperature. Very recently, Abel and Mahesha [23] considered the effects of buoyancy and variable thermal conductivity in a power law fluid past on a vertical stretching sheet in the presence of non-uniform heat source.

In the mentioned papers investigators restrict their analyses to MHD flow and heat transfer over a stretching sheet. However the intricate flow and heat transfer problem with the effects of internal heat generation/absorption, viscous dissipation, work done by stress, and the thermal radiation is yet to be studied. This has applications to several industrial problems (say engineering processes involving nuclear power plants, gas turbines, and many others, [24, 25]). In all these studies, the thermo-physical properties of the ambient fluids were assumed to be constant. However it is well known that these properties may change with temperature, especially the thermal conductivity. Available literature on variable thermal conductivity [26-30] shows that this type of flow has not been investigated for power law fluids in the presence of suction/bowing and impermeability of the stretching sheet.

In view of these applications, we study the unsteady flow and heat transfer phenomena in a power law fluid over a porous stretching surface, in the presence of the influence of an external transverse magnetic field in a porous medium, taking into account the internal heat generation/absorption, viscous dissipation, work done by stress, variable thermal conductivities, variable viscosities, and thermal radiation. This is a generalization of Andersson *et al*. [20] work to the case of power law fluid flow and heat transfer where the thermal conductivity is a function of temperature in the presence of transverse magnetic field. Recently, flow of non-Newtonian polymer solution was investigated by Savvas *et al.* [31] and it was shown that computer simulation is a powerful technique to predict the flow behavior. Because of the complexity and non-linearity of our problem, the resulting equations are solved numerically by the Keller-Box method. One of the important observations of the study is that suction reduces the horizontal velocity where as blowing increases the horizontal velocity for all values of power law index.

The results obtained herein, are compared with the solutions by Prasad and Vajravelu [32] which also studied heat transfer in the MHD flow of a power law fluid over a non-isothermal stretching sheet in absence of each of the unsteadiness parameter, *i. e.* $A = 0$ the porous medium, *i. e.* $S = 0$, the temperature buoyancy parameter, *i. e.*, and variable viscosity = constant, to check the accuracy.

Hence, the objective of present paper is to study the above mentioned unsteady flow and heat transfer in an incompressible laminar, electrically conducting and non-Newtonian fluid over a non-isothermal stretching sheet with the variation in the viscosity and thermal conductivity in a porous medium by the influence of an external transverse magnetic field which have been obtained and studied numerically. Numerical results are presented for velocity and temperature profiles for different parameters of the problem as power law parameter, unsteadiness parameter, radiation parameter, magnetic field parameter, porous medium parameter, temperature buoyancy parameter, Prandtl parameter, modified Eckert parameter, Joule heating parameter, and heat source/sink parameter, *etc*. In addition, the effects of the pertinent parameters on the skin friction and the rate of heat transfer are also discussed.

Mathematical analysis

Consider a viscous, unsteady 2-D flow of an incompressible, electrically conducting power law fluid in the presence of an external transverse magnetic field of strength $B(x, t)$ over a stretching sheet lying on the plane $y > 0$. The flow is confined to $y > 0$ (for details see [20]). The thermo-physical properties of the sheet and the viscosity of the fluid vary as assumed to be $\mu(x, t) = \mu_0 b^{-3} x^{(1-n)/n}(1 - \gamma t)^3$ at which μ_0 is the viscosity at temperature T_w, b and γ are positive constants with dimension reciprocal time. The fluid motion arises due to the stretching of the elastic sheet in a porous medium. The momentum and energy equations for a fluid with variable thermal conductivities and variable viscosities in the presence of internal heat generation/absorption, viscous dissipation and thermal radiation are studied.

The u and v are the velocity of x and y components, T is the temperature. Under these assumptions, the governing boundary layer equations of continuity, momentum, and energy under Boussinesq approximations could be written as:

– the equation of continuity

$$\frac{\partial u}{\partial x}+\frac{\partial v}{\partial y}=0 \tag{1}$$

– the equation of momentum

$$\frac{\partial u}{\partial t}+u\frac{\partial u}{\partial x}+v\frac{\partial u}{\partial y}=-\frac{1}{\rho}\frac{\partial}{\partial y}\left(-\mu(x,t)\frac{\partial u}{\partial y}\right)^{n}-\frac{\sigma B^{2}u}{\rho}+g\beta(T-T_{\infty})-\frac{\nu}{K}u \tag{2}$$

– the equation of energy

$$\frac{\partial T}{\partial t}+u\frac{\partial T}{\partial x}+v\frac{\partial T}{\partial y}=\frac{1}{\rho c_p}\frac{\partial}{\partial y}\left(\alpha(T,t)\frac{\partial T}{\partial y}\right)-\frac{1}{\rho c_p}\frac{\partial q_r}{\partial y}+$$
$$+\frac{Q}{\rho c_p}(T-T_{\infty})+\frac{1}{\rho c_p}\left(\mu(x,t)\frac{\partial u}{\partial y}\right)^{n+1}+\frac{\sigma B^{2}}{\rho c_p}u^{2} \tag{3}$$

The initial and boundary conditions are

$$\begin{aligned}&t<0: \quad u=v=T=0, \quad \text{for all points } (x,y)\\ &t\geq 0: \quad u(x,0)=U_{\mathrm{w}}(x,t), \quad v(x,0)=v_{\mathrm{w}}(x,t), \quad T(x,0)=T_{\mathrm{w}}(x,t), \quad x\geq 0\\ &t\geq 0: \quad u(x,\infty)=0 \quad T(x,\infty)=T_{\infty}\end{aligned} \tag{4}$$

Following Andersson *et al.* [33], the stretching velocity $U_{\mathrm{w}}(x, t)$ is assumed to be $U_{\mathrm{w}}(x, t) = bx/(1-\gamma t)$ and the velocity $v_{\mathrm{w}}(x, t)$ across the stretching sheet is assumed to be $v_{\mathrm{w}}(x, t) = (1-\gamma t)R/b$ in which it is a suction velocity when $v_{\mathrm{w}} < 0$ and it is blowing velocity when $v_{\mathrm{w}} > 0$. We have b as the initial stretching rate and $b/(1-\gamma t)$ is increasing with time. In the context of polymer extrusion, the material properties particularly the elasticity of the extruded sheet may vary with time even though the sheet is being pulled by a constant force.

With unsteady stretching, however, γ^{-1} becomes the representative time scale of the resulting unsteady boundary layer problem. We assume that all of the surface temperature $T_{\mathrm{w}}(x, t)$, the applied transverse magnetic field $B(x, t)$, the expansion coefficient of temperature $\beta(x, t)$, the volumetric heat generation/absorption rate $Q(x, t)$, and the porous medium $\Im(x, t)$, are on a stretching sheet to vary with the distance x along the sheet and time in the following forms:

$$\begin{gathered}B(x,t)=B_0\frac{1}{\sqrt{1-\gamma t}}, \quad \beta(x,t)=\beta_0\frac{1}{1-\gamma t}, \quad Q(x,t)=Q_0\frac{1}{1-\gamma t}\\ T_{\mathrm{w}}(x,t)=T_{\infty}+A_1\left(\frac{x^2}{l^2}\right)\frac{1}{1-\gamma t}, \quad \Im(x,t)=\frac{\nu}{K}=S_0\frac{1}{1-\gamma t}\end{gathered} \tag{5}$$

where B_0 is the uniform magnetic field acting normal to the plate, g – the gravitational acceleration, β_0, Q_0, and A_1 are constants which depend on the properties of the fluid, l – a characteristic length, ρ, μ, T_{∞} and c_p are the density, dynamic viscosity, the free stream temperature, and the specific heat at constant pressure, respectively.

The subscripts w and ∞ stand for the wall and free stream conditions, $\alpha(T, t)$ is the temperature-dependent thermal conductivity. We consider the temperature-dependent thermal conductivity in the following form [26]:

$$\alpha(T,t)=\alpha_\infty(1-\gamma t)^3\left(1+\varepsilon\frac{T-T_\infty}{\Delta T}\right) \tag{6}$$

where ε is a small parameter, $\Delta T = T_w - T_\infty$, T_w – the given temperature at the wall, and α_∞ – the thermal conductivity of the fluid far away from the sheet. The term containing Q represents the temperature-dependent heat source when $Q > 0$ and heat sink when $Q < 0$; and it deals, respectively, with the situations of exothermic and endothermic chemical reactions. The third and fourth terms on the right-hand side of eq. (3) represent, respectively, the viscous dissipation and the ohmic heating effect. The last term q_r on the right-hand side of eq. (3) represents the radiative heat flux. Using the Rosseland approximation ([34, 35]), the radiative heat flux q_r could be expressed by:

$$q_r=-\frac{4\sigma^*}{3k^*}\frac{\partial T^4}{\partial y} \tag{7}$$

where the σ^* represents the Stefan-Boltzman constant and k^* is the Rosseland mean absorption coefficient.

Assuming that the temperature difference within the flow is sufficiently small such that T^4 could be approached as the linear function of temperature:

$$T^4 \cong 4T_\infty^3 T - 3T_\infty^4 \tag{8}$$

The equation of continuity is satisfied if we choose a stream function $\psi(x, y)$ such that $u = \partial\psi/\partial y$ and $v = -\partial\psi/\partial x$. The governing partial differential eqs. (1)-(3) admit similarity solutions for obtaining the dimensionless stream function $f(\eta)$ and temperature $\theta(\eta)$. The relative parameters are introduced as:

$$\psi=\frac{x}{b}(1-\gamma t)f(\eta),\quad \eta=b^2\frac{1}{(1-\gamma t)^2}y,\quad T=T_\infty+T_0 bx\frac{1}{(1-\gamma t)}\theta(\eta) \tag{9}$$

After introducing the similarity transformation, the eqs. (2)-(3) can be transformed into a set of following forms in terms with $f(\eta)$ and $\theta(\eta)$, expressed as:

$$n(-f'')^{n-1}f''' + ff'' - f'^2 - A[f' + 2\eta f''] - (M+S)f' + G\theta = 0 \tag{10}$$

$$(k_0+\delta\,\mathrm{Pr}+\varepsilon\theta)\theta'' + \varepsilon\theta'^2 - A\,\mathrm{Pr}(\theta+2\eta\theta') + \mathrm{Pr}(f\theta' - f'\theta) + \beta\theta + \mathrm{Pr}(E_c f''^{(n+1)} + Jf'^2) = 0 \tag{11}$$

with the appropriate boundary conditions:

$$\begin{aligned}&\eta=0; \quad f(0)=R,\quad f'(0)=1,\quad \theta(0)=1,\\ &\eta\to\infty; \quad f'(\infty)=0,\quad \theta(\infty)=0\end{aligned} \tag{12}$$

where the prime denotes a partial differentiation with respect to η, $k_0 = xA_1/T_0bl^2$ is a constant parameter, R is the introduced to represent the surface mass transfer which is positive for blowing, negative for suction, and shows that, the suction or blowing parameter R is used to control the strength and direction of the normal flow at the boundary.

Skin-friction coefficient and Nusselt number

The parameters of engineering interest for the present problem are the local skin-friction coefficient and the local Nusselt number which indicate the physical wall shear stress and rate of heat transfer, respectively.

The equation defining the wall skin-friction is given by:

$$\tau_w = -\left(-\mu(x,t)\frac{\partial u}{\partial y}\right)^n_{y=0}$$

The skin-friction coefficient is given by, eq. (13):

$$C_\text{f} = -\frac{\tau_\text{w}}{x\mu_0^n} = [-f''(0)]^n \tag{13}$$

Now the heat flux (q_w) at the wall is given by;

$$q_w = -\alpha(T,t)\left(\frac{\partial T}{\partial y}\right)_{y=0}$$

Hence the Nusselt number is obtained by eq. (14):

$$\text{Nu} = \frac{A_1 q_w}{\alpha_\infty T_0^2 b^4 l^2 (k_0 + \varepsilon)} = -\theta'(0) \tag{14}$$

Numerical computations

The system of non-linear ordinary differential eqs. (10) and (11) together with the boundary conditions (12) are locally similar and solved numerically by using the sixth order of Runge-Kutta integration accompanied with the shooting iteration scheme. We have chosen a step size of $\Delta\eta = 0.01$ to satisfy the convergence criterion of 10^{-6} in all cases. The value of η_∞ was found for each iteration loop by $\eta_\infty = \eta_\infty + \Delta\eta$. The maximum value of η_∞ for each group of parameters n, A, M, S, G, k_0, δ, ε, Pr, β, Ec, R and J is determined when the value of the unknown boundary conditions at $\eta = 0$ is not changed to successful loop with error less than 10^{-6}.

In order to verify the effects of the step size ($\Delta\eta$) we ran the code for our model with three different step sizes as $\Delta\eta$ = 0.01, $\Delta\eta$ = 0.004 and $\Delta\eta$ = 0.001 and in each case we found excellent agreement among them. Figure 1 shows the velocity profiles for different step sizes.

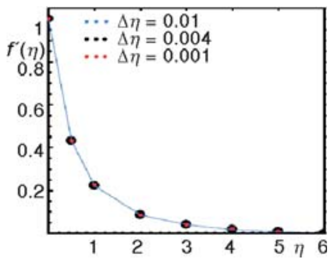

Figure 1. Velocity profiles for different step sizes

Results and discussion

In order to gain physical insight the velocity, temperature and concentration profiles have been discussed by assigning numerical values to the parameter encountered in the problem in which the numerical results are tabulated and displayed with the graphical illustrations.

In order to verify the accuracy of our present method, we have compared our results with those of Prasad and Vajravelu [32] and Andersson *et al.* [20]. Table 1 shows the values of $-f''(0)$ for various values of n. The comparisons in all above cases are found to be excellent and agreed, also, the results are found to be similar to Prasad and Vajravelu [32] and Andersson *et al*. [20], so it is good.

Table 1. Comparison of the values – $f''(0)$ with Prasad and Vajravelu [32] and Andersson *et al.* [20]

n	Prasad and Vajravelu [32]	Andersson *et al.* [20]	Present study
0.4	1.273	1.27968	1.27498
0.6	1.096	1.09838	1.09612
1.0	1.000	1.00000	1.00000
1.2	0.987	0.98738	0.98721
1.5	0.981	0.98058	0.98032
2.0	0.980	0.98035	0.98007

Table 2. Numerical values of the skin-friction coefficient (C_f) and Nusselt number Nu at the plate surface with *n*

n	A	M	S	G	R	Pr	Ec	β	J	δ	C_f	Nu
0.2	0.1	1.0	0.2	0.0	0.0	1.0	0.5	0.0	0.1	0.1	1.3635	0.9406
0.4											1.4631	1.1063
0.8											1.4925	1.2118
1.0											1.4825	1.2310
1.4											1.4546	1.2462
1.8											1.4281	1.2481

Figures 2(a) and 2(b), display the velocity and temperature profiles under the different power law parameter. The velocity increases, while the temperature profiles decrease with increasing power law parameter.

Figures 3(a) and 3(b), display the velocity and temperature profiles under the different unsteadiness parameter. The velocity and the temperature profiles increase with increasing unsteadiness parameter. Figures 4(a) and 4(b) , it is clear that the velocity decreases, while the temperature profiles increase with the increase of the magnetic parameter.

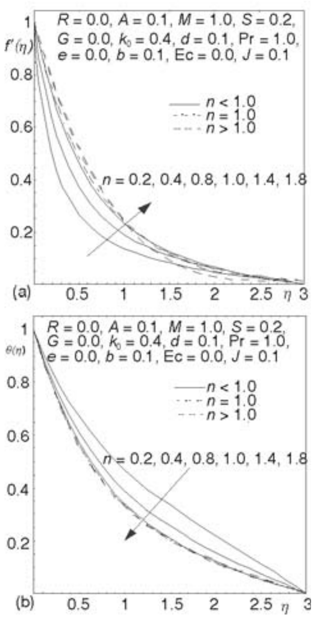

Figure 2. Effect of power law parameter on (a) the velocity profile and (b) the temperature profile

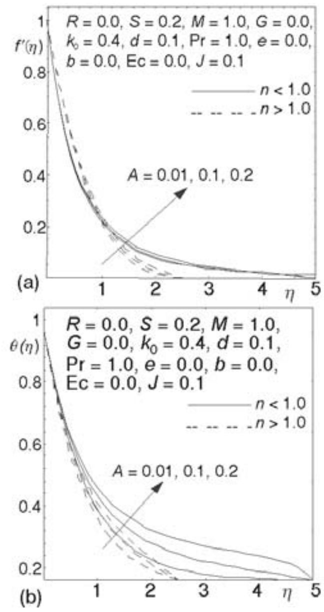

Figure 3. Effect of unsteadines parameter on (a) the velocity profile and (b) the temperature profile

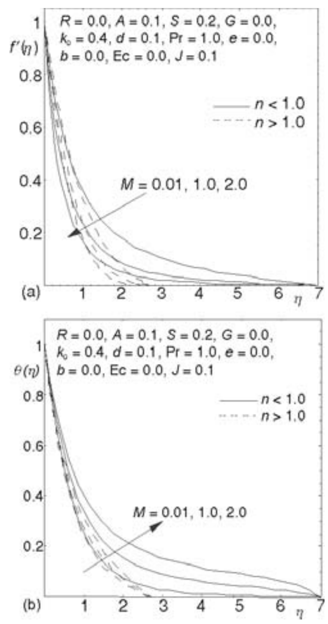

Figure 4. Effect of magnetic parameter on (a) the velocity profile and (b) the temperature profile

Figures 5(a) and 5(b) , show the effects of porous medium parameter on the velocity and temperature profiles; also, we found that the velocity decreases, but the temperature profiles increase with the increase of porous medium parameters. Figures 6(a) and 6(b) , show the effects of temperature buoyancy parameter on the velocity and temperature profiles; also, we found that the velocity and the temperature profiles increase in case $n < 1.0$, but decrease in case $n > 1.0$ with the increase of temperature buoyancy parameters. Figures 7(a) and 7(b) , show the effects of surface mass transfer parameter on the velocity and temperature profiles; also, we found that the velocity and the temperature profiles decrease with the increase of surface mass transfer parameters. *i. e.* The thermal boundary layer becomes thicker for suction and thinner for blowing.

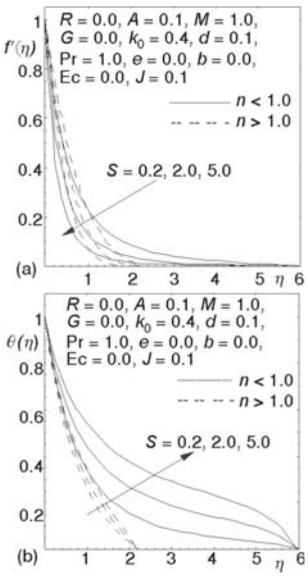

Figure 5. Effect of porous medium parameter on (a) the velocity profile and (b) the temperature profile

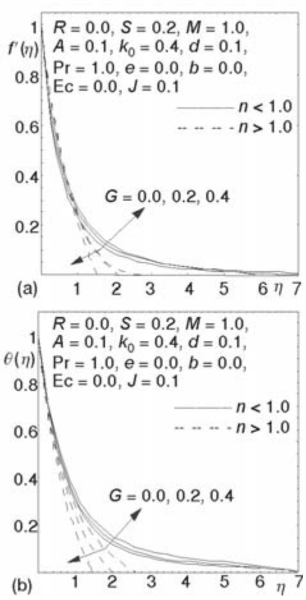

Figure 6. Effect of the temperature buoyancy parameter on (a) the velocity profile and (b) the temperature profile

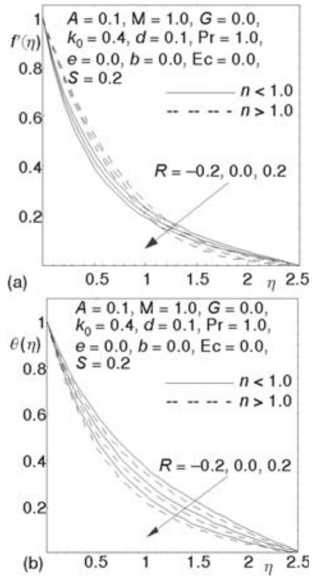

Figure 7. Effect of surface mass transfer parameter on (a) the velocity profile and (b) the temperature profile

The effects of Pr on the velocity and the temperature profiles are shown in fig. 8(a) and 8(b), respectively. It is observed that the velocity profile increases, while the temperature profile decreases with the increase of Prandtl number. Physically, the thermal boundary layer thickness decreases with the increase of the values of Prandtl number. The effects of modified Eckert parameter on the velocity and the temperature profiles are shown in figs. 9(a) and 9(b), respectively. It is observed that the velocity profile decreases, while the temperature profile increases with the increase of modified Eckert parameter. This is in conformity with that fact that energy is stored in the fluid region as a consequence of dissipation due to viscosity and elastic deformation.

Figure 10, shows the effects of heat source/sink parameter on temperature profile; also, we found that the temperature profile increases with the increase of heat source/sink parameters. The effects of Joule heating parameter on the velocity and the temperature profiles are shown in figs. 11(a) and 11(b), respectively. It is observed that the velocity and the temperature profiles increase with the increase of Joule heating parameters. The effects of δ on the velocity

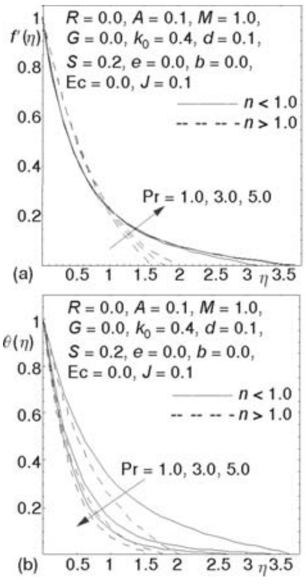

Figure 8. Effect of Prandtl number on (a) the velocity profile and (b) the temperature profile

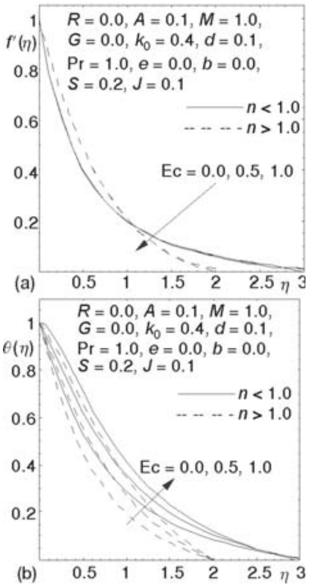

Figure 9. Effect of modified Eckert parameter on (a) the velocity profile and (b) the temperature profile

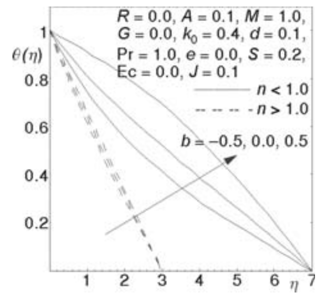

Figure 10. Effect of heat source/sink parameter on the temperature profile

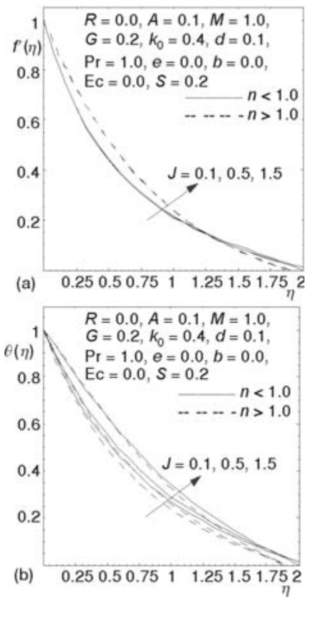

Figure 11. Effect of Joule heating parameter on (a) the velocity profile and (b) the temperature profile

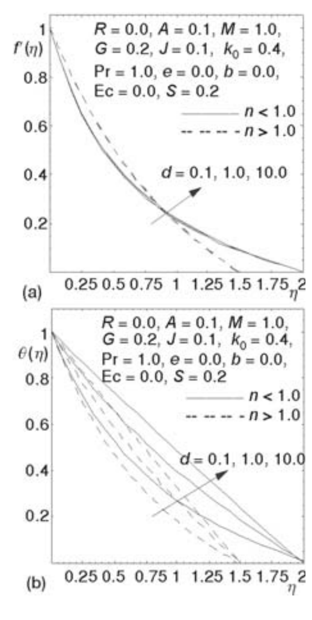

Figure 12. Effect of radiation parameter on (a) the velocity profile and (b) the temperature profile

and the temperature profiles are shown in figs. 12(a) and 12(b), respectively. It is observed that the velocity and the temperature increase with the increasing radiation parameter.

From tab. 1, an increase for power law gives an increase in the value of the dimensionless quantities $-f''(0)$. In addition, by comparing our results with those of Prasad and Vajravelu [32] and Andersson *et al.* [20], the results are found to be similar, so it is good.

The numerical values of the Skin-friction and the Nusselt number are given in tabs. 2. and 3. It may be noted that with an increase in the power law parameter n, we observe that the Skin-friction coefficient increases in case of $n < 1$, while decreases in case of $n > 1$ and the Nusselt number increases. Also, with the increase in the unsteadiness parameter A, we observe that the Skin-friction coefficient increases in case of $n < 1$, while decreases in case of $n > 1$ and the Nusselt number decreases.

Both at $n < 1$ and $n > 1$, for an increase in each of the magnetic parameter M, porous medium parameter S and Modified Eckert parameter Ec, we observe that the Skin-friction coefficient increases and the Nusselt number decreases. While, with an increase in the temperature buoyancy parameter G, we observe that the Skin-friction coefficient decreases and the Nusselt number increases.

Table 3. Numerical values of the skin-friction coefficient (C_f) and Nusselt number (Nu) at the plate surface with A, M, S, G, R, Pr, Ec, β, J, δ, and n

A	M	S	G	R	Pr	Ec	β	J	δ	C_f		Nu	
										n = 0.6	n = 1.6	n = 0.6	n = 1.6
0.01	1.0	0.2	0.0	0.0	1.0	0.5	0.0	0.1	0.1	1.4867	1.4494	1.2969	1.3811
0.1										1.4884	1.4412	1.244	1.3644
0.2										1.4918	1.4348	1.2621	1.3562
0.1	0.01	0.2	0.0	0.0	1.0	0.5	0.0	0.1	0.1	1.1809	1.0055	1.3947	1.4239
	1.0									1.4884	1.4412	1.2644	1.3644
	2.0									1.7166	1.7103	1.0929	1.3053
0.1	1.0	0.2	0.0	0.0	1.0	0.5	0.0	0.1	0.1	1.4884	1.4412	1.2644	1.3644
		2.0								1.8680	1.7148	1.0929	1.3055
		5.0								2.3073	2.1098	0.9280	1.2246
0.1	1.0	0.2	0.0	0.0	1.0	0.5	0.0	0.1	0.1	1.4884	1.4412	1.2644	1.3644
			0.2							1.4283	1.3656	1.2913	1.3957
			0.4							1.3701	1.3434	1.3058	1.4312
0.1	1.0	0.2	0.0	–0.2	1.0	0.5	0.0	0.1	0.1	1.4121	1.3321	1.1075	1.1668
				0.0						1.4884	1.4415	1.2644	1.3644
				0.2						1.5842	1.5576	1.5116	1.5936
0.1	1.0	0.2	0.0	0.0	1.0	0.5	0.0	0.1	0.1	1.4884	1.4412	1.2644	1.3644
					3.0					1.4987	1.4528	2.0260	2.1348
					5.0					1.4996	1.4686	2.3604	2.4702
0.1	1.0	0.2	0.0	0.0	1.0	0.0	0.0	0.1	0.1	1.4764	1.4302	1.3341	1.7324
						0.5				1.4884	1.4412	1.2644	1.3644
						1.0				1.5816	1.5610	0.8715	0.9312
0.1	1.0	0.2	0.0	0.0	1.0	0.5	–0.5	1.0	10.0			0.3090	0.4383
							0.0					0.2194	0.3945
							0.5					0.0983	0.3472
0.1	1.0	0.2	0.0	0.0	1.0	0.5	0.0	0.1	0.1	1.4884	1.4412	1.2644	1.3644
								0.5		1.4847	1.3681	1.1585	1.1991
								1.5		1.4397	1.3586	0.8089	0.6763
0.1	1.0	0.2	0.0	0.0	1.0	0.5	0.0	0.1	0.1	1.4884	1.4412	1.2644	1.3644
									1.0	1.4021	0.8329	0.9743	
									100.0	1.4329	1.3958	0.2194	0.3945

It may be noted that with an increase in the surface mass transfer parameter R and Prandtl number, we observe that the skin-friction coefficient and the Nusselt number increase. While the skin-friction coefficient and the Nusselt number decrease with increasing the Joule heating parameter J and radiation parameter δ. With an increase in the heat source/sink parameter β, we found that the value of the Nusselt number decreases, *i. e.* for positive β we have a heat source in the boundary layer when $T_w < T_\infty$ and a heat sink when $T_w < T_\infty$. Physically these correspond, to the recombination and dissociation within the boundary layer, respectively. For the case of a cooled wall ($T_w < T_\infty$), there is heat transfer from the fluid to the wall even without heat source. The presence of a heat source $\beta > 0$ will further increase the heat flow to the wall. When β is negative, this indicates a heat source for ($T_w > T_\infty$) and a heat sink ($T_w < T_\infty$). This corresponds to combustion and an endothermic chemical reaction. For the case of heated wall ($T_w > > T_\infty$), the presence of a heat source creates a layer of hot fluid adjacent to the surface and therefore heat at the wall decreases. For the cooled wall case ($T_w < T_\infty$), the presence of a heat sink blankets the surface with a layer of cool fluid, and hence the heat flow at the surface decreases.

Conclusions

In this work the unsteady flow and heat transfer in an incompressible laminar, electrically conducting and non-Newtonian fluid over a non-isothermal stretching sheet with the variation in the viscosity and thermal conductivity in a porous medium by the influence of an external transverse magnetic field have been obtained and studied numerically. The main conclusions are:

- The effect of increasing values of the magnetic parameter and the porous medium parameter is to decrease the momentum boundary layer thickness and to increase the thermal boundary layer thickness.
- The effect of increasing values of the variable viscosity parameter and the temperature buoyancy parameter is to increase the momentum boundary layer as well as the thermal boundary layer thickness.
- The effect of increasing values of the Prandtl number is to increase the momentum boundary layer thickness and to decrease the thermal boundary layer thickness . For an increase in the unsteadiness parameter, the skin-friction coefficient increases in case of $n < 1$, while decreases in case of $n > 1$ and the Nusselt number decreases.
- For an increase in each of the magnetic field parameter, the porous medium parameter and modified Eckert parameter, skin friction increases, but the rate of heat transfer decreases. While with an increase in the temperature buoyancy parameter, the skin-friction coefficient decreases and the Nusselt number increases.
- Of all the parameters considered, the variable viscosity parameter has the strong effect on the drag, heat transfer characteristics, the velocity and the temperature field in the boundary layer of a non-linearly stretching sheet.

Nomenclature

A – unsteady parameter, (= γ/b)
A_1 – constant
B_0 – magnetic field
b – stretching rate, a positive constant
C_f – skin friction
c_p – specific heat at constant pressure, [JK^{-1}]
Ec – modified Eckert number [= $A_1^2 x^4/l^4 b^2 c_p T_0 (T_w - T_\infty)^2$]
f – dimensionless velocity
G – temperature buoyancy parameter (= $g\beta_0 T_0/b$)
g – gravitational acceleration, [ms^{-2}]
J – Joule heating parameter (= $\sigma B_0^2 l^2 (T_w - T_\infty)/T_0 b \rho c_p A_1 x^2$)
J – Joule effect
K – consistency coefficient
K^* – mean absorption coefficient
l – characteristic length, [m]
M – magnetic parameter (= $\sigma B_0^2/\rho b$)
n – power law index
Nu – Nusselt number
p – pressure, [Nm^{-2}]
Pr – modified Prandtl number (= $\rho c_p A_1/\alpha_\infty T_0 b^3 l^2$)
Q – internal heat generation/absorption, [Wm^{-3}]

q_w – local heat flux at the sheet, [Wm^{-2}]
q_r – radiative heat flux, [Wm^{-2}]
R – surface mass transfer
S – porous medium parameter (= S_0/b)
T – temperature distribution, [K]
T_w – temperature at the sheet, [K]
T_∞ – temperature of the fluid at infinity, [K]
ΔT – sheet temperature (= $T_w - T_\infty$)
t – time, [s]
U – velocity of the sheet, [ms^{-1}]
u – velocity in the x-direction, [ms^{-1}]
v – velocity in the y-direction, [ms^{-1}]
x – horizontal distance, [m]
y – vertical distance, [m]

Greek symbols

$\alpha(T, t)$ – thermal conductivity, [WKm^{-1}]
α_∞ – thermal conductivity at infinity, [WKm^{-1}]
β – heat source/sink parameter (= $A_1Q_0/b^4\alpha_\infty T_0l^2$)
$\beta(x,t)$ – heat source/sink parameter
δ – thermal radiation parameter (= $16\sigma^*b^3l^6(T_w - T_\infty)^3/3k^*\rho c_pA_1^2x^5$)
ε – small parameter
η – similarity variable
θ – dimensionless temperature distribution
$\mu(x,t)$ – kinematic viscosity of the power law fluid, [$kgm^{-1}s^{-1}$]
ρ – density, [kgm^{-3}]
σ – electrical conductivity
σ^* – Stephan-Boltzmann constant
τ – shear stress
ψ – stream function, [m^2s^{-1}]

Subscripts

w, ∞ – conditions at the surface and in the free stream

References

[1] Sakiadis, B. C., Boundary Layer Behavior on Continuous Solid Surfaces, *AIChE J., 7* (1961), 1, pp. 26-28
[2] Crane, L. J., Flow Past a Stretching Plate, *ZAMP, 21* (1970), pp. 645-647
[3] Afzal, N., Varshney, I. S., The Cooling of a Low Heat Resistance Stretching Sheet Moving through a Fluid, *Warme Stoffubertrag, 14* (1980), 4, pp. 289-293
[4] Banks, W. H. H., Similarity Solutions of the Boundary Layer Equations for a Stretching Wall, *J. Mec. Theor. Appl., 2* (1983), 3, pp. 375-392
[5] Chen, C. K., Char, M. I., Heat Transfer of a Continuous Stretching Surface with Suction or Blowing, *J. Math. Anal. Appl., 135* (1988), 2, pp. 568-580
[6] Gupta, P. S., Gupta, A. S., Heat and Mass Transfer on a Stretching Sheet with Suction or Blowing, *Can. J. Chem. Eng., 55* (1977), 6, pp. 744-746
[7] Vleggaar, J., Laminar Boundary Layer Behaviour on Continuous Accelerating Surfaces, *Chem. Eng. Sci., 32* (1977), 12, pp. 1517-1525
[8] Grubka, L. J., Bobba, K. M., Heat Transfer Characteristics of a Continuous Stretching Surface with Variable Temperature, *ASME J. Heat Transfer, 107* (1985), 1, pp. 248-250
[9] Sarpakaya, T., Flow on Non-Newtonian Fluids in a Magnetic Field, *AIChE J., 7* (1961), 2, pp. 324-328
[10] Andersson, H. I., MHD Flow of a Visco-Elastic Fluid Past a Stretching Surface, *Acta Mech., 95* (1992), 1-4, pp. 227-230
[11] Sam Lawrence, P., Nageswara Rao, B., Heat Transfer in the MHD Flow of a Viscoelastic Fluid over a Stretching Sheet, *ZAMM, 77* (1997), 4, pp. 317-319
[12] Abel, M. S., *et al.*, Heat Transfer in MHD Visco-Elastic Fluid Flow over a Stretching Surface, *ZAMM, 81* (2001), 10, pp. 691-698
[13] Chowdhury, M. K., Islam, M. N., MHD Free Convection Flow of Visco-Elastic Fluid Past an Infinite Vertical Porous Plate, *Heat Mass Transfer, 36* (2000), 5, pp. 439-447
[14] Khan, S. K., *et al*., Visco-Elastic MHD Flow, Heat and Mass Transfer over a Porous Stretching Sheet with Dissipation Energy and Stress Work, *Heat Mass Transfer, 40* (2003), 1-4, pp. 47-57
[15] Abel, M. S., Mahesha, N., Heat Transfer in MHD Visco-Elastic Fluid Flow over a Stretching Sheet with Variable Thermal Conductivity, Non-Uniform Heat Source and Radiation, *Appl. Math. Model., 32* (2008), 10, pp. 1965-1983
[16] Char, M. I., Heat and Mass Transfer in a Hydromagnetic Flow of the Visco-Elastic Fluid over a Stretching Sheet, *J. Math. Anal. Appl., 186* (1994), 3, pp. 674-689
[17] Schowalter, W.R., The Application of Boundary Layer Theory to Power Law Pseudo Plastic Fluids: Similar Solutions, *AIChE J., 6* (1960), 1, pp. 24-28

[18] Acrious, A., *et al*., Momentum and Heat Transfer in Laminar Boundary Layer Flow on Non-Newtonian Fluids Past External Surfaces, *AIChE J., 6* (1960), 1, pp. 312-316
[19] Lee, S. Y., Ames, W. F., Similar Solutions for Non-Newtonian Fluids, *AIChE J., 12* (1966), 4, pp. 700-708
[20] Andersson, H. I., *et al.*, Magnetohydrodynamic Flow of a Power Law Fluid over a Stretching Sheet, *Int. J. Nonlinear Mech., 72* (1992), 4, pp. 929-936
[21] Howell, T. G., *et al*., Momentum and Heat Transfer on a Continuous Moving Surface in a Power Law Fluid, *Int. J. Heat Mass Transfer 40* (1997), 8, pp. 1853-1861
[22] Hassanien, I. A., *et al*., Flow and Heat Transfer in a Power Law Fluid over a Non-Isothermal Stretching Sheet, *Math. Comput. Model. 28* (1998), 9, pp. 105-116
[23] Abel, M. S., Mahesha, N., Effects of Thermal Buoyancy and Variable Thermal Conductivity in a Power Law Fluid Past a Vertical Stretching Sheet in the Presence of Non Uniform Heat Source, *Int. J. Nonlinear Mech. 44* (2009), 1, pp. 1-12
[24] Vajravelu, K., Flow and Heat Transfer in a Saturated Porous Medium over a Stretching Surface, *ZAMM, 74* (1994), 12, pp. 605-614
[25] Vajravlu, K., Nayfeh, J., Convective Heat Transfer at a Stretching Sheet, *Acta Mech., 96* (1993), 1-4, pp. 47-54
[26] Chaim, T. C., Heat Transfer in a Fluid with Variable Thermal Conductivity over a Linearly Stretching Sheet, *Acta Mech., 129* (1998), 1-2, pp. 63-72
[27] Chiam, T. C., Heat Transfer with Variable Thermal Conductivity in a Stagnation Point Flow Towards a Stretching Sheet, *Int. Commun. Heat Mass Transfer, 23* (1996), 2, pp. 239-248
[28] Datti, P. S., *et al.*, MHD Visco-Elastic Fluid Flow over a Non-Isothermal Stretching Sheet, *Int. J. Eng. Sci., 42* (2004), 8-9, pp. 935-946
[29] Prasad, K. V., *et al.*, Momentum and Heat Transfer in Visco-Elastic Fluid Flow in a Porous Medium over a Non-Isothermal Stretching Sheet, *Int. J. Numer. Meth. Heat Fluid Flow, 10* (2000), 8, pp. 786-802
[30] Abel, M. S., *et al*., Buoyancy Force and Thermal Radiation Effects in MHD Boundary Layer Visco-Elastic Fluid Flow over Continuously Moving Stretching Surface, *Int. J. Therm. Sci., 44* (2005), 5, pp. 465-476
[31] Savvas, T. A., *et al*., On the Flow of Non-Newtonian Polymer Solutions, *Appl.Math. Model., 18* (1994), 1, pp. 14-21
[32] Prasad, K. V., Vajravelu, K., Heat Transfer in the MHD Flow of a Power Law Fluid over a Non-Isothermal Stretching Sheet, *Int. J. Heat and Mass Transfer, 52* (2009), 21-22, pp. 4956-4965
[33] Andersson, H. I., *et al*., Flow of a Power-Law Fluid Film on an Unsteady Stretching Surface, *J. Non-Newtonian Fluid Mech., 62* (1996), 1, pp. 1-8
[34] Sparrow, E. M., Cess, R. D., *Radiation Heat Transfer*, Brooks/Cole, Belmont, Cal., USA, 1970
[35] El-Arabawy, H. A. M., Effect of Suction/Injection on the Flow of a Micropolar Fluid Past a Continuously Moving Plate in the Presence of Radiation, *Int. J. Heat Mass Transfer, 46* (2003), 8, pp. 1471-1477

Paper submitted: May 29, 2011
Paper revised: January 7, 2012
Paper accepted: February 8, 2012